OFFICE OF NAVAL RESEARCH

Contract No. N00014-91-J-1409

Technical Report No. 120

The Evaluation of Rate Constants for Rapid Electrode Reactions by using Microelectrode Voltammetry: Virtues of Measurements at Lower Temperatures

by

Lance K. Safford and Michael J. Weaver

Prepared for Publication

in the

Journal of Electroanalytical Chemistry

Purdue University

Department of Chemistry

West Lafayette, Indiana 47907

February 1992

SECURITY CLASSIFICATION OF THIS PAGE

REPORT DOCUMENTATION PAGE

Form Approved
OMB No. 0704-0188

1a. REPORT SECURITY CLASSIFICATION Unclassified	1b. RESTRICTIVE MARKINGS
2a. SECURITY CLASSIFICATION AUTHORITY	3. DISTRIBUTION/AVAILABILITY OF REPORT Approved for public release and sale; its distribution is unlimited.
2b. DECLASSIFICATION/DOWNGRADING SCHEDULE	
4. PERFORMING ORGANIZATION REPORT NUMBER(S) Technical Report No. 120	5. MONITORING ORGANIZATION REPORT NUMBER(S)
6a. NAME OF PERFORMING ORGANIZATION Purdue University Department of Chemistry 6b. OFFICE SYMBOL (If applicable)	7a. NAME OF MONITORING ORGANIZATION Division of Sponsored Programs Purdue Research Foundation
6c. ADDRESS (City, State, and ZIP Code) Purdue University Department of Chemistry West Lafayette, IN 47907	7b. ADDRESS (City, State, and ZIP Code) Purdue University West Lafayette, IN 47907
8a. NAME OF FUNDING/SPONSORING ORGANIZATION Office of Naval Research 8b. OFFICE SYMBOL (If applicable)	9. PROCUREMENT INSTRUMENT IDENTIFICATION NUMBER Contract No. N00014-91-J-1409
8c. ADDRESS (City, State, and ZIP Code) 800 N. Quincy Street Arlington, VA 22217	10. SOURCE OF FUNDING NUMBERS PROGRAM ELEMENT NO. / PROJECT NO. / TASK NO / WORK UNIT ACCESSION NO.

11. TITLE (Include Security Classification)
The Evaluation of Rate Constants for Rapid Electrode Reactions by using Microelectrode Voltammetry: Virtues of Measurements at Lower Temperatures

12. PERSONAL AUTHOR(S)
Lance K. Safford and Michael J. Weaver

13a. TYPE OF REPORT	13b. TIME COVERED	14. DATE OF REPORT (Year, Month, Day)	15. PAGE COUNT
Technical	FROM _____ TO _____	February 28, 1992	

16. SUPPLEMENTARY NOTATION

17. COSATI CODES			18. SUBJECT TERMS (Continue on reverse if necessary and identify by block number)
FIELD	GROUP	SUB-GROUP	electrochemical kinetic measurements at lower temperatures, cyclic voltammetric measurements, redox couples in acetone, propionitrile, and butyronitrile

19. ABSTRACT (Continue on reverse if necessary and identify by block number)

The prospects of utilizing electrochemical kinetic measurements at lower temperatures for evaluating reliably the standard rate constants, k_s, of rapid redox couples in nonaqueous media, specifically using microelectrode voltammetry, have been examined by means of digital simulations along with experiment. Cyclic voltammetric measurements were made between 200 and 300K at a gold microdisk, for ferrocenium–ferrocene ($Fc^{+/o}$), o-nitrotoluene$^{o/-}$, and nitromesitylene$^{o/-}$ redox couples in acetone, propionitrile, and butyronitrile, at a gold microdisk with scan rates from 100 to 10^4 V s^{-1}. The latter two couples were selected as examples of systems that exhibit rapid, yet still unambiguously measurable, k_s values at ambient temperatures; the more facile $Fc^{+/o}$ system has been suspected to yield immeasurably fast electrode kinetics using conventional techniques under these conditions. Sample simulated voltammograms were generated between 200 and 300K for a sequence of activation enthalpies for electron exchange, $\Delta H^{\ddagger}_{ex}$, accounting also for known temperature-dependent

20. DISTRIBUTION/AVAILABILITY OF ABSTRACT ☐ UNCLASSIFIED/UNLIMITED ☐ SAME AS RPT. ☐ DTIC USERS	21. ABSTRACT SECURITY CLASSIFICATION
22a. NAME OF RESPONSIBLE INDIVIDUAL	22b. TELEPHONE (Include Area Code) / 22c. OFFICE SYMBOL

DD Form 1473, JUN 86 *Previous editions are obsolete.* SECURITY CLASSIFICATION OF THIS PAGE

Accession For	
NTIS GRA&I	☑
DTIC TAB	☐
Unannounced	☐
Justification	
By	
Distribution/	
Availability Codes	
Dist	Avail and/or Special
A-1	

(19. cont.)

diffusion coefficients, solution resistance, and double-layer capacitance. As long as $\Delta H^{\ddagger}_{ox}$ > 10 kJ mol^{-1}, the use of diminished temperatures in such solvents is predicted to facilitate the reliable evaluation of k_s. This expectation is in harmony with experiment: k_s for $Fc^{+/o}$ is apparently readily evaluated at lower temperatures, yielding $\Delta H^{\ddagger}_{ox} \approx 20$ kJ mol^{-1}. The temperature-dependent electrode kinetic data for $Fc^{+/o}$ are compared briefly with some expectations of contemporary theory.

ABSTRACT

The prospects of utilizing electrochemical kinetic measurements at lower temperatures for evaluating reliably the standard rate constants, k_s, of rapid redox couples in nonaqueous media, specifically using microelectrode voltammetry, have been examined by means of digital simulations along with experiment. Cyclic voltammetric measurements were made between 200 and 300K at a gold microdisk, for ferrocenium–ferrocene ($Fc^{+/o}$), o-nitrotoluene$^{o/-}$, and nitromesitylene$^{o/-}$ redox couples in acetone, propionitrile, and butyronitrile, at a gold microdisk with scan rates from 100 to 10^4 V s^{-1}. The latter two couples were selected as examples of systems that exhibit rapid, yet still unambiguously measurable, k_s values at ambient temperatures; the more facile $Fc^{+/o}$ system has been suspected to yield immeasurably fast electrode kinetics using conventional techniques under these conditions. Sample simulated voltammograms were generated between 200 and 300K for a sequence of activation enthalpies for electron exchange, $\Delta H^{\ddagger}_{ex}$, accounting also for known temperature-dependent diffusion coefficients, solution resistance, and double-layer capacitance. As long as $\Delta H^{\ddagger}_{ex} > 10$ kJ mol^{-1}, the use of diminished temperatures in such solvents is predicted to facilitate the reliable evaluation of k_s. This expectation is in harmony with experiment: k_s for $Fc^{+/o}$ is apparently readily evaluated at lower temperatures, yielding $\Delta H^{\ddagger}_{ex} \approx$ 20 kJ mol^{-1}. The temperature-dependent electrode kinetic data for $Fc^{+/o}$ are compared briefly with some expectations of contemporary theory.

The evaluation of rate constants for rapid electrochemical exchange reactions is a quest with a history that has been in some respects almost as frustrating as it is venerable. A variety of electrochemical relaxation techniques have been employed over the years, leading to the accumulation of an extensive body of kinetic data for reversible redox couples. From time to time, however, the reliability of such data for rapid reactions has been called into question. The kernel of the problem is simple. Solute mass transport rates to and from electrode surfaces in most experimental configurations tend to be comparable to, or slower than, heterogeneous electron-transfer rates for many simple redox couples. This factor, when combined with the deleterious effects of solution resistance and instrumental nonidealities, can make the reliable evaluation of electrode kinetics an extremely tortuous undertaking.

In recent years, microelectrodes have become popular as a means of ameliorating these difficulties, especially when used in conjunction with cyclic voltammetry.[1] Specifically, their extremely small surface areas both enhance the effective mass transport rates and diminish the magnitude of the resistive solution potential drop. In addition, the combined effects of a smaller solution resistance, R_s, and double-layer capacitance, C_{dl}, enable very rapid potential sweep rates to be employed, thereby further enhancing mass transport rates. At least for microelectrodes of conventional size, however, the residual resistance-capacitance effects can complicate or vitiate the measurement of standard rate constants for rapid electrode reactions, say $k_s \gtrsim 1\text{-}2$ cm s^{-1}, even in polar solvents containing high supporting-electrolyte concentrations.[2] Since many outer-sphere electrochemical exchange reactions are known (or anticipated) to exhibit such large k_s values at ambient temperatures, their evaluation by microelectrode voltammetry, as by other methods, can be far from straightforward.

Nevertheless, the difficulties inherent in such measurements might be

anticipated to be eased considerably by judicious alterations in the experimental conditions. One such modification is to diminish the temperature. Since heterogeneous electron transfer even in the absence of inner-shell reorganization should feature activation energies typically in the range 20-25 kJ mol^{-1} (vide infra), one anticipates that substantial diminutions in k_s should accrue by this means, thereby facilitating in principle its reliable evaluation. The use of nonaqueous solvents such as butyronitrile to pursue electrochemical measurements down to 150K was demonstrated twenty years ago.[3] More recently, there has been considerable use of cyclic voltammetry at low temperatures to examine reactive electrogenerated species.[4-9] Surprisingly, however, there has been only sporadic interest in performing electrochemical kinetic measurements at diminished temperatures[10-13], especially for rapid reversible redox couples.[14] This inactivity stands in contrast to the well-known use of lower-temperature environments for exploring other areas of reactive electron-transfer chemistry.

Nonetheless, microelectrode cyclic voltammetry would appear to be particularly well suited to the evaluation of electrode kinetics at lower temperatures, in that the major impediment to such measurements arising from enhanced solution resistance can be accounted for effectively (as well as being minimized) by this technique. Described herein is an experimental examination of this issue by means of fast-scan cyclic voltammetry at gold microelectrodes for a series of test redox systems, together with predicted voltammetric responses from digital simulation. The latter tactic is invaluable not only for extracting rate constants from voltammetric data over a wide range of sweep rates in the face of significant solution resistance and other experimental nonidealities[2], but also for predicting the measurability of electrode kinetics as a function of system conditions, including temperature. The primary objective is to ascertain whether such tactics can be beneficial to the reliable evaluation

of rapid electrode kinetics, and as a hoped-for consequence improve the confidence in ambient-temperature evaluations of k_s for facile redox couples.

The specific systems chosen here are ferrocenium-ferrocene ($Fc^{+/o}$), and o-nitrotoluene and nitromesitylene molecule-radical anion redox couples ($o\text{-}Nt^{o/-}$ and $Nm^{o/-}$), in acetone, propionitrile, and butyronitrile solvents. These solvents remain liquid throughout the temperature range of interest here, and also are anticipated to exert relatively straightforward effects on the electron-transfer dynamics (vide infra). The three redox couples were selected since their rate constants at ambient temperatures in the three solvents range from values that are easily (and unambiguously) evaluated by microelectrode cyclic voltammetry, ca 0.3-0.5 cm s^{-1} ($Nm^{o/-}$), to those, ca 3-5 cm s^{-1} ($Fc^{+/o}$), that approach (or even may surpass) the limit of measurability. Indeed, such k_s values for $Fc^{+/o}$ commonly obtained by contemporary methods are sufficiently large to cast some doubt on even their approximate validity. This suspicion has been heightened recently by a widely publicized report of much larger k_s values, around 200 cm s^{-1}, obtained for $Fc^{+/o}$ in acetonitrile at platinum microelectrodes having sizes apparently approaching nanometer dimensions.[15]

Evaluating k_s for $Fc^{+/o}$ at lower temperatures by using conventional microelectrode voltammetry, as pursued here, provides a means by which the ambient-temperature behavior of this archetypical "fast" redox couple can be appraised anew (cf ref. 14). Each redox couple/solvent system was examined in the present work over a sufficient sub-ambient temperature range, 200-300K, so to depress k_s by substantial factors (up to 30-50 fold) and thereby facilitate its measurement. Comparing the temperature-dependent behavior of the three redox couples alongside simulated voltammograms obtained for experimentally relevant values of R_s, C_{dl}, and k_s enables the virtues (and likely pitfalls) associated with the evaluation of electrode kinetics at lower temperatures to be assessed in some detail.

EXPERIMENTAL SECTION

The potentiostat used for microelectrode studies was a modified version of a previously published design.[16] Moderately fast ($\nu < 20{,}000$ V s^{-1}) scan rates could be employed without incurring distortions due to the band-pass of the potentiostat. The potentiostat was driven with waveforms output from an Hewlett-Packard 3314A Function Generator. Experimental traces were captured by a Tektronix 2430A Digital Storage Oscilloscope and transferred to a Zenith-80386 personal computer via a standard GPIB (IEEE-488) interface bus.

Low-temperature studies were conducted with a home-built cryostat. The electrochemical cell was inserted in to a Teflon jacket through which thermostatted gaseous N_2 was passed. The cell temperature was monitored by use of a fine Teflon-coated thermocouple immersed in the electrolyte solution. Temperature control was accomplished by first cooling the gaseous N_2 by passage through a heat exchanger immersed in liquid N_2. The pre-cooled gas was then heated to the desired temperature by passage over a resistance coil heater controlled in a feedback mode by a Varian Temperature Controller. With this system, thermal stability was ±1°C over periods of more than an hour, and equilibrium at each temperature was reached within 3-4 minutes.

Three solvents were used in this study. Acetone (Fischer) (fp = 179 K) was dried over $CaSO_4$ and distilled fresh prior to each experiment. Propionitrile (Aldrich) (fp = 180 K) was passed down a column of activated neutral alumina and then distilled twice from CaH_2. Butyronitrile (Aldrich) (fp = 161 K) was treated as propionitrile but distillation was carried out at reduced pressure. These solvents were chosen for their low freezing points and low solution resistances over the range of temperature employed. The range of useful temperatures was determined both by the solvent freezing point and by the ability to observe stable voltammograms over the period, 5 to 7 minutes, necessary to acquire data

over a full range of scan rates from 20 to 10,000 V s^{-1}.

Tetraethylammonium hexafluorophosphate ($TEAH_6$) was prepared by the metathesis of tetraethylammonium bromide (Et_4NBr) with ammonium hexafluorophosphate (NH_4PF_6) (Aldrich) in acetone, and recrystallized twice from absolute ethanol. Tetrabutylammonium hexafluorophosphate (TBAH) was prepared in a similar manner by the metathesis of tetrabutylammonium iodide with NH_4PF_6. Both salts were dried at 398 K for 24 hours and stored in a desiccator prior to use. o-Nitrotoluene (Aldrich) was distilled under reduced pressure, nitromesitylene (Aldrich) was recrystallized from absolute ethanol, and ferrocene (Aldrich) was sublimed before use.

The auxiliary electrode was a small coil of platinum wire that was flame annealed prior to introduction to the cell. A home-made ferrocenium/ferrocene reference electrode was used, constructed by placing a frit made from polymerized Kasil #1 (The PQ Corporation; Valley Forge, PA) in the end of a 6 mm O.D. glass tube. The barrel of the tube was filled with the solvent-supporting electrolyte solution du jour and a small amount of an equimolar mixture of ferrocene and ferricenium hexafluorophosphate. A freshly annealed platinum wire was then placed in the solution inside the electrode barrel and the top was sealed with a rubber septum. This arrangement produced a reference electrode that was stable for several days under normal conditions, or 2-3 weeks if kept in an inert atmosphere.[17] In the variable temperature experiments, the reference electrode was placed in a separate thermostatted holder remote from the cell. Electrical connection between the reference compartment and the working cell was achieved by a section of thin Teflon tubing filled with solution.

The 5μm radius gold microelectrodes used in this study were either constructed in house by means of published methods[18] or purchased from bioanalytical Systems, Inc. (West Lafayette, IN). The two types of electrodes

yielded similar results. Platinum electrodes of the same origins were also used. The day-to-day reproducibility of k_s values obtained using Pt electrodes, however, was often considerably inferior to that of gold. Consequently, all the voltammetric data reported herein were acquired at gold microelectrodes. Prior to use, the electrode was polished on successively finer grades of Al_2O_3 (Buehler Ltd.) (1 μm - 0.05 μm), sonicated in pure water and finally in solvent/supporting-electrolyte solution for a minimum of 5 minutes each.

Measurements of R_s were accomplished by AC impedance, over the frequency range 50-500 Hz, using a 0.95 cm diameter Au disk electrode, pretreated in a similar manner as the microdisks. It was inserted into the cell such that the solvent meniscus covered the face of the electrode. The equipment used for these measurements included a EG&G Princeton Applied Research Model 173 Potentiostat with a Model 179 Digital Coulometer, a Model 175 Universal Programmer, a Model 5204 Lock-in-Analyzer, and an HP 3314A Function Generator. In-phase and quadrature currents were recorded on a Soltec X-T-Y-Ý chart recorder.

RESULTS AND DISCUSSION

Simulated temperature-dependent voltammetry

Contrary to common belief, the solution resistance can exert a significant distorting influence upon voltammograms obtained at conventional size (ca 5 μm radius) microelectrodes, especially at high potential scan rates.[2,19] (See ref. 2 for citations of earlier literature.) While analytical treatments of electrode kinetics under these conditions are only of limited utility at microelectrodes, such effects along with the coupled influence of the double-layer capacitance can be assessed in detail by means of digital-simulation techniques. As a prelude to outlining the experimental voltammetric data, we describe the results of corresponding digital simulations aimed at examining the measurability of electrode kinetics over the temperature range 200-300K from microelectrode

voltammetry.

Two distinct, yet complementary, simulation procedures were employed here. When conditions were such that the effects of radial diffusion were minor, as encountered at high scan rates, an approach based on the Hopscotch algorithm[20,21] was utilized.[19] For lower scan rates where radial diffusion to the microelectrode is more important (or even dominant), a two-dimensional algorithm based on the "conformal-map" method[22] provides a suitably efficient procedure in this computationally more demanding regime. Together, these two procedures enable the coupled effects of solution resistance, double-layer capacitance, and finite electrode kinetics upon microelectrode voltammetry to be assessed throughout the range of scan rates encompassing the liner diffusion and steady-state mass transfer regimes. (See refs. 2 and 17 for relevant procedural details.)

As the temperature is diminished, k_s will inevitably decrease since heterogeneous electron exchange is necessarily an activated process. This will result in an increased contribution to the irreversible nature of the voltammetric response, as reflected most simply in the cathodic-anodic peak separation, and thereby should aid the evaluation of k_s. Two other factors, however, tend to mitigate against this straightforwardly desirable situation. First, the rate of diffusional mass transport as determined by the diffusion coefficient D will also decreases as the temperature is lowered, thereby diminishing the extent to which electrode kinetics can influence the voltammetric response. In addition, the solution resistance will increase under these conditions, enhancing the degree of distortion of the voltammetric waveshape.

At least in the linear diffusion limit (i.e., at high scan rates ν), the ease of measurability of k_s (at a given ν) is given by $k_s D^{-\frac{1}{2}}$.[23,24] Aside from solution resistance effects, then, the kinetic measurability should increase towards lower temperatures provided that the activation enthalpy for reactant

diffusion, $\Delta H_D^{\ddagger}$, is less than twice that for the heterogeneous electron exchange process, $\Delta H_{ex}^{\ddagger}$. Given that $\Delta H_D^{\ddagger}$ for the present systems is roughly 10–14 kJ mol^{-1} (vide infra), enhancing the measurability of k_s by the tactic of lowering the temperature on the basis only requires that $\Delta H_{ex}^{\ddagger} > 5$–7 kJ mol^{-1}. This is a very mild requirement: as shown below, markedly larger $\Delta H_{ex}^{\ddagger}$ values, ca 15–25 kJ mol^{-1}, are both predicted and observed even for facile outer-sphere redox couples.

It is nonetheless useful to examine simulated voltammetric responses as a function of temperature that account for solution resistance as well as reactant diffusion effects. Figure 1 summarizes some pertinent results plotted as cathodic–anodic peak potential separations, ΔE_p, obtained from simulated voltammograms obtained over the temperature range 200–300 K. The specific simulation conditions are: electrode radius = 5μm, reactant concentration = 1m$\underline{M}$, $D = 10^{-5}$ cm^2 s^{-1} (at 298K), number of electrons n = 1, scan rate ν = 1 kV s^{-1}, and $\Delta H_D^{\ddagger}$ = 15 kJ mol^{-1}. The bottom (dotted) trace in Fig. 1 shows the temperature-dependent ΔE_p values anticipated in the "ideal reversible" limit, where $k_s \rightarrow \infty$ and $R_s = 0$. Since largely linear diffusion is encountered at the fast scan rate chosen, these ΔE_p values are essentially equal to 2.2RT/F.[23] The dashed curve in Fig. 1 is obtained for $k_s \rightarrow \infty$, but accounting for the presence of temperature-dependent solution resistance as would be encountered for butyronitrile containing 0.1 $\underline{M}$ TBAH. (The parameters chosen were a solution resistivity, ρ, of 140 Ω cm at 298K, with a temperature coefficient described by an Arrhenius activation energy, $\Delta H_{\rho}^{\ddagger}$, of 15 kJ mol^{-1}. As for the $\Delta H_D^{\ddagger}$ value chosen above, this $\Delta H_{\rho}^{\ddagger}$ value corresponds to an upper limit, "worst case", example.) Unlike the "ideal" dotted curve, this dashed trace exhibits ΔE_p values that increase with decreasing temperature, reflecting the enhanced distorting effect of the solution resistance under these conditions. As expected, then, in the absence of a more complete analysis, such behavior could easily be mistaken for finite temperature-

dependent electrode kinetics.

The three solid traces, labelled a-c in Fig. 1, were generated by including the presence of finite electrode kinetics as well as solution resistance. In each case, the standard rate constant at 298K is set at 5 cm s^{-1}, with the activation enthalpy $\Delta H^{\ddagger}_{ex}$ taken as 10, 25, and 40 kJ mol^{-1} in a, b, and c, respectively. The electrochemical transfer coefficient, α, was assumed to be constant and equal to 0.5. Selecting such a large k_s value at room temperature yields only a small "kinetic" contribution to ΔE_p, $\Delta(\Delta E_p)_k \simeq 10$ mV, this could easily by masked by the larger component of the voltammetric peak separation due to solution resistance, $\Delta(\Delta E_p)_R$, at least in butyronitrile. For the smallest $\Delta H^{\ddagger}_{ex}$ value (curve c), no advantage in the evaluation of k_s is afforded by diminishing the temperature since $\Delta(\Delta E_p)_k$ is seen to remain largely invariant while $\Delta(\Delta E_p)_R$ increases significantly under these conditions (Fig. 1). Nevertheless, for larger $\Delta H^{\ddagger}_{ex}$ values, including those anticipated for typical "fast" redox couples, substantial enhancements in the degree of kinetic information are afforded towards lower temperatures. Thus for $\Delta H^{\ddagger}_{ex} = 25$ kJ mol^{-1} (curve b), ΔE_p is seen to increase markedly under these conditions, so that $\Delta(\Delta E_p)_k \approx 120$ mV at 200K (Fig. 1). It is therefore apparent that this tactic can provide substantial benefits in the evaluation of electrode kinetics by means of microelectrode voltammetry, even in the face of sufficient resistance-based distortions so to vitiate such analyses at ambient temperatures.

Also of interest in this regard is the effect of varying the scan rate, ν, on the kinetic measurability at a given temperature. Figure 2 summarizes the results of illustrative simulations of this type, in the form of plots of ΔE_p versus $\log(\nu^{-\frac{1}{2}})$, calculated at 298 and 198K for the conditions used in Fig. 1. The solid traces labelled a and c are obtained at 298 and 198K, respectively, in the presence of solution resistance (appropriate for 0.1 M butyronitrile

electrolyte). The increase in ΔE_p seen towards higher scan rates arising from resistive distortions is especially evident at the lower temperature. The dashed trace b is obtained at 298K for k_s = 5 cm s^{-1}. As anticipated, this curve is only displaced slightly from trace a (for $k_s \rightarrow \infty$), even at the highest scan rate, $\nu = 10^4$ V s^{-1} in Fig. 1, indicating that the kinetics are barely measurable under these conditions. The three dotted traces (d-f) refer to 198K, with k_s set at 0.65, 0.02, and 7 x 10^{-4} cm s^{-1}, respectively. (These k_s values arise from choosing k_s = 5 cm s^{-1} at 298K, with $\Delta H^{\ddagger}_{ox}$ values of 10, 25, and 40 kJ mol^{-1}, as before.) Comparison of traces d-f with the corresponding "reversible limit" trace c shows again the presence of substantial ($\gtrsim$ 0.1 V) $\Delta(\Delta E_p)_k$ values for the two larger activation energies. These large kinetic effects are aided by, but not limited to, the use of relatively rapid potential scan rates.

These considerations point straightforwardly to the advantages of lower temperatures for electrode kinetics measurements. At least one qualification to this seemingly rosy picture is prompted however, by examining the simulated voltammograms themselves. Figure 3 displays such a set of temperature-dependent voltammograms at 10^3 V s^{-1}, employing the same conditions used in Fig. 1, and with k_s = 5 cm s^{-1} at 298K, $\Delta H^{\ddagger}_{ox}$ = 20 kJ mol^{-1}. The temperature ranges from 298K (outermost voltammogram) to 198K in equal decrements. Although the enhanced cathodic-anodic peak separations towards lower temperatures signal primarily an enhanced measurability of electrode kinetics, also evident are the diminished faradaic currents relative to the nonfaradaic (double-layer charging) background. Consequently, then, the more sluggish diffusional transport occurring at lower temperatures mitigates against the extraction of the desired faradaic information versus the nonfaradaic background, especially at higher scan rates. In principle, this situation can be eased by employing higher reactant concentrations and/or lower scan rates; however, solubility constraints may restrict this

tactic, which also enhances the degree of resistive distortions. A related difficulty, noted below, concerns the occurrence of additional background currents towards lower temperatures arising from adsorption of solute species and/or adventitious impurities.

Experimental voltammetry

As already noted, the nitroaromatic molecule–radical anion redox couples o-nitrotoluene ($o\text{-}Nt^{o/-}$) and especially nitromesitylene ($Nm^{o/-}$) were selected here since they exhibit standard rate constants in acetonitrile and other simple polar solvents that can be arranged to fall in the range, ca 0.2–1 cm s^{-1}, at ambient temperature that, while still rapid, can be evaluated with some confidence by using contemporary methods,[25] including microelectrode voltammetry. Additionally, k_s for such molecule–radical anion systems can be diminished substantially by employing larger tetraalkylammonium supporting electrolyte cations (for example, see ref. 28). Exploring the temperature-dependent voltammetric behavior of these systems in tandem with corresponding measurements for the more facile ferrocenium–ferrocene ($Fc^{+/o}$) couple provides a useful means of assessing the reliability of the latter data.

The experimental tactics involved obtaining cyclic voltammograms for a wide range of scan rates, 10^2 – 10^4 V s^{-1}, at 20 deg. intervals over the temperature range 200–300K. Providing satisfactory reproducibility was attained, each scan rate–dependent set of experimental data was analyzed by comparison with corresponding voltammograms simulated using appropriate values of R_s, C_{dl}, D, and k_s. The R_s values were extracted from the measured solution resistivities, ρ, by means of the well-known relation

$$R_s = \rho/4r \qquad (1)$$

where r is the microelectrode radius. The required temperature-dependent ρ values for the electrolyte solutions employed here summarized in Table I. (These

values are in good agreement with the earlier measurements of Bowyer et al.,[29] given in parentheses in Table I. For convenience, ρ values obtained in acetonitrile containing 0.3 M TBAH are also included. The effective double-layer capacitance, C_{dl}, was extracted from the magnitude of the voltammetric currents prior to the onset of the faradaic wave. These values were generally seen to lie within the range 15–20 $\mu F\ cm^{-2}$ for the present solvent systems, and are insensitive to the temperature, decreasing by only 2–3 $\mu F\ cm^{-2}$ from 300 to 200K. The diffusion coefficient, D, for each system were extracted from the diffusion-limiting current, i_d, obtained for the steady-state voltammogram at the gold microelectrode by using[31]

$$i_d = 4nFaDC^\circ \qquad (2)$$

where C° is the reactant solution concentration. The resulting temperature-dependent D values, along with the effective Arrhenius activation energies for diffusion, $\Delta H_D^\ddagger$, are summarized in Table II.

Knowledge of these parameters enabled the degree of electrode kinetic information contained in the cyclic voltammograms to be evaluated with some confidence. Briefly, the appropriate values of R_s, C_{dl}, D, along with ν and C° were input into the simulational algorithm, and the input trial k_s values varied in order to obtain the best fit between the simulated and experimental voltammetric data (cf ref. 32). The visual fit was obtained by overlaying these data on a terminal screen, and involved matching the entire current-potential cycle, rather than just the cathodic-anodic peak separation, ΔE_p. This procedure yielded an "optimal" k_s value, $k_s(opt)$, for each scan rate and temperature. As a check on the reliability of the result, a pair of additional simulated voltammograms were then generated using k_s values equal to $0.5k_s(opt)$ and $2k_s(opt)$. If no clearcut change in the voltammetric waveshape was discerned, the true k_s value was deemed to lie beyond the measurable region under the particular

conditions (ν,T) chosen, and the result was rejected.

In some cases, especially for nitromesitylene$^{o/-}$ at lower temperatures, the electrode kinetics are sufficiently sluggish so that the voltammetric waves encompass a substantial (> 0.1 - 0.2 V) range of cathodic and anodic overpotentials. In order to extract reliable k_s values under these conditions, it is desirable to include the likely potential dependence of the transfer coefficient, α, in the simulations.[27,29,33,34] The form of $\alpha(E)$ employed here is the usual relation[35] (see also Appendix to ref. 36):

$$\alpha = 0.5 \pm F(E - E_f)/2\lambda \qquad (3)$$

where E_f is the formal potential of the redox couple, λ is the so-called intrinsic reorganization energy, and the plus/minus sign refers to cathodic and anodic transfer coefficients, respectively. To achieve the best fit for Nm$^{o/-}$ in butyronitrile from 238 to 298K, for example, $d\alpha/dE$ equalled about 0.43 V^{-1}, corresponding to λ = 110 kJ mol^{-1}. This value is closely similar to that deduced earlier for Nm$^{o/-}$.[33]

Following the simulational analysis presented in the preceding section, it is useful to express the degree of electrode kinetic information contained in a given cyclic voltammogram in terms of the additional peak separation, $\Delta(\Delta E_p)_k$, beyond that corresponding to the limit where $k_s \rightarrow \infty$. Table III summarizes representative $\Delta(\Delta E_p)_k$ values (mV) as a function of scan rate and temperature for 3 mM Fc$^{+/o}$ in acetone, propionitrile, and butyronitrile, and for 3.5 mM o-Nt$^{o/-}$ in the latter two solvents. (The nitroaromatic redox couples yielded less reliable data in acetone, probably due to the effects of residual water.)

Examination of the results for Fc$^{+/o}$ at 298K show that in most cases, especially in acetone, the $\Delta(\Delta E_p)_k$ are sufficiently small, $\lesssim$ 20 mV, to make the reliable extraction of k_s values fraught with difficulty. At 198K, by contrast, the corresponding $\Delta(\Delta E_p)_k$ values are sufficiently large, $\gtrsim$ 100 mV, even at

moderate scan rates (~ 1KV s^{-1}) so to ease considerably the evaluation of k_s. A similar trend is also observed for o-$Nt^{o/-}$, although satisfactorily large $\Delta(\Delta E_p)_k$ values are also observed at the higher temperature (Table III). Results from a related experimental data set, specifically for $Fc^{+/o}$ (circles), o-$Nt^{o/-}$ (squares), and $Nm^{o/-}$ (triangles) in butyronitrile containing 0.3 M TBAH, are summarized in Fig. 4 in the form of plots of ΔE_p versus T, for a given scan rate (1kV s^{-1}). The corresponding ΔE_p – T plot for $k_s \rightarrow \infty$ is shown as a dashed line (cf Fig. 1). This plot shows clearly how the degree of electrode kinetic information for all three redox couples, adjudged from the vertical displacement between the solid and dashed lines, increases markedly as the temperature is decreased below ambient values.

Self-consistent k_s values (within 10–20%) were usually obtained at a given temperature by analyzing the voltammogram over a suitable range of scan rates, such that significant kinetic information is available. The resulting "best-fit" k_s values obtained in this fashion are summarized in Table IV. Note that the k_s values for $Fc^{+/o}$ at ambient temperatures, especially in acetone and propionitrile, are sufficiently large ($\gtrsim$ 3 cm s^{-1}), to render their evaluation under these conditions extremely tenuous. Strong evidence for at least their approximate validity (k_s within ca 2-fold), however, is deduced by extrapolating in Arrhenius-fashion the k_s values obtained at lower temperatures, say below 250K, where the rates are depressed sufficiently to render their evaluation by microelectrode voltammetry significantly more trustworthy. A comparable k_s value, ca 3.5 cm s^{-1}, was obtained for $Fc^{+/o}$ at 298K in acetonitrile as that observed here in acetone,[17] although the temperature-dependent analysis was restricted to T $\gtrsim$ 250K by the higher freezing point of acetonitrile.

It is also worth noting in this context that comparable $\Delta H^{\ddagger}_{ox}$ values are obtained for $Fc^{+/o}$, ca 20 kJ mol^{-1}, as those for the significantly more sluggish

nitroaromatic couples, ca 25 kJ mol^{-1} (Table IV). Recalling the arguments in the preceding section, and in particular Fig. 1, it is this degree of thermal activation required for outer-sphere electron exchange that enables electrochemical measurements at lower temperatures to provide a potent tactic for evaluating the heterogeneous reaction rates. Some further interpretation of the activation parameters is provided below.

Even though this temperature-dependent analysis can therefore be deemed successful, it is necessary to point out that the use of lower temperatures can trigger additional experimental difficulties beyond those normally encountered at ambient temperatures. In particular, we found it necessary to pay even greater attention to solvent, electrolyte, and reactant purity when undertaking rate measurements at temperatures approaching 200K. Time-dependent distortion of voltammetric waveshapes was often encountered under these conditions, attributed to slow adsorption of adventitious impurities. Along with rigorous purification procedures, these difficulties were minimized (and hopefully eliminated) by employing freshly polished electrodes, and comparing the first and last set of voltammetric scans at a given temperature, acquired under identical conditions.

Kinetic Consequences

Although this study is concerned primarily with the practical matter of evaluating rapid rate constants, it is nonetheless of interest to examine briefly the fundamental implications of the resulting temperature-dependent rate data. First, the slower electron-exchange kinetics of the nitroaromatic couples relative to $Fc^{+/o}$ are reflected largely in significantly (ca 5 kJ mol^{-1}) larger $\Delta H^{\ddagger}_{ex}$ values for the former (Table IV). Besides these activation enthalpies, Table IV also lists apparent preexponential factors for electron exchange, A_{ex}, obtained from the usual expression

$$k_s = A_{ex} \exp(-\Delta H^{\ddagger}_{ex}/RT) \quad (4)$$

The A_{ex} values for the nitroaromatic couples are seen to be comparable to, or larger than, those for $Fc^{+/o}$. The larger activation enthalpies for the former may be due to contributions from both inner- and outer-shell reorganization components.[28]

While more quantitative interpretation of the rate parameters are thwarted by several uncertainties, not the least of which are possible electrostatic double-layer and other environmental effects, it is useful to consider further the ferrocenium-ferrocene rate data. This is justified in part by our earlier observation, supported by measurements in the present study, that k_s for such metallocene ($Cp_2M^{+/o}$) couples are insensitive to the electrostatic double-layer structure.[37] We have earlier undertaken extensive studies of solvent-dependent electron exchange kinetics of various $Cp_2M^{+/o}$ couples with M = Fc, Co, both at electrode surfaces[38-41] and in homogeneous solution.[42-50] A major motivation for these studies concerns the elucidation of dynamical solvent effects upon electron-transfer kinetics. The metallocenes offer several major attributes for this purpose, including their solubility (and relative freedom from ion pairing) in a variety of polar media, roughly spherical geometry, and a typically small contribution from inner-shell (i.e., reactant intramolecular) reorganization to the overall activation barrier. (See refs. 49 and 50 for overviews.) For ferrocenium-ferrocene electrochemical exchange, the inner-shell contribution to the enthalpic barrier, ΔH^{*}_{is}, is only about 1.5 kJ mol^{-1} (see footnote 47 of ref. 46; note that the electrochemical ΔH^{*}_{is} value is one half of that for homogeneous-phase self exchange).

The present rate constants and activation parameters are quite similar to those obtained for $Fc^{+/o}$ over a comparably large temperature range by Baranski et al at Pt-nonaqueous interfaces using ac impedance.[14] They are also comparable

to activation-parameter data for several other metallocene couples obtained similarly at Hg-nonaqueous interfaces over a narrower temperature range, reported earlier from this laboratory.[39] A common feature of all these results is that both the rate constants and activation enthalpies for $Cp_2M^{+/o}$ couples at metal-polar nonaqueous interfaces are comparable to the predictions of the conventional dielectric continuum treatment presuming that reactant-electrode imaging interactions are small or negligible. We have discussed this issue earlier in connection with other related topics.[39,40,50]

To illustrate this point in the present context, Table V compares the activation enthalpies for $Fc^{+/o}$ electrochemical exchange measured here with values of the activation free energy, ΔG^*_{cont}, as extracted from the usual dielectric continuum formula for outer-shell reorganization[35]:

$$\Delta G^*_{os} = (e^2/8)[a^{-1} - (2R_e)^{-1}]\ (\epsilon_{op}^{-1} - \epsilon_s^{-1}) \qquad (5)$$

Here e is the electronic charge, a is the reactant radius, R_e is the reactant-electrode distance in the transition state, and ϵ_{op} and ϵ_s are the solvent optical and static dielectric constants, respectively. As before,[39,40] a is taken as 0.38 pm, and $R_e \rightarrow \infty$; i.e., electrode imaging is neglected. The ΔG^*_{cont} values were obtained from these ΔG^*_{os} estimates by adding the inner-shell component, 1.5 kJ mol^{-1}. Comparison between the experimental $\Delta H^{\ddagger}_{ex}$ and calculated ΔG^*_{cont} values (ignoring entropic and related effects for the moment) shows them to be comparable, although the latter are slightly (4.5 kJ mol^{-1}) larger. Significantly, however, the $\Delta H^{\ddagger}_{ex}$ values are markedly larger than the ΔG^*_{cont} values, ca 12 kJ mol^{-1}, that would be obtained in the limit where $a = R_e$, i.e., where reactant-electrode imaging is complete.

It might be argued that this and related earlier findings[14,39] indicates that the reaction site for the metallocenes is sufficiently far from the metal surface so that $2R_e >> a$. While this may be the case, a more sophisticated

theoretical treatment including the effects of metal field penetration (both with and without solvent spatial correlations) predicts that such stabilizing reactant–surface interactions will largely be absent for $2R_e - a$, and can even become destabilizing (i.e., *increase* ΔG^*) under some conditions.[51,52]

At least two other complicating features are worth mentioning here. First, even in the absence of imaging effects there are good reasons to expect that the actual activation free energy will differ significantly from the ususal dielectric–continuum estimates. The most direct evidence comes from optical electron–transfer measurements in symmetrical mixed–valence compounds, for which the desired reorganization energies can be obtained directly.[53] Binuclear ferrocenium–ferrocene complexes provide a valuable means by which such information can be obtained for the present reaction.[54–56] While the departures of the experimental reorganization energies in polar solvents from the dielectric–continuum predictions are not large ($\lesssim$ 20–25%), the former tend to be smaller.[56] Such noncontinuum solvent effects can be accounted for semiquantitatively in terms of simple molecular–based models.[51,56] On this basis, then, the measured activation energies can be deemed to be satisfactorily close to (within ca 10–20% of) the ΔG^* values anticipated in the absence of reactant–electrode imaging.

A second complicating feature, however, concerns the anticipated relationship of the temperature–dependent rate measurements to theoretical activation energies. Strictly speaking, the measured activation energy for the overall reaction, $\Delta H^{\ddagger}_{ex}$, may differ from the activation free energy for the electron–transfer step, ΔG^*, due either to the presence of a significant enthalpic work term, and/or to a nonzero activation entropy, ΔS^*, for electron transfer. According to the dielectric–continuum model, $T\Delta S^* \approx 0$ ($\lesssim$ 1 kJ mol^{-1} at room temperature).[57] A comparable result is also obtained from an entropic

analysis which accounts for the experimentally known departures in the zero-frequency (Born charging) component of the activation energy from the dielectric-continuum model.[39,57] An additional, perhaps more important, contribution to $\Delta H_{ex}^{\ddagger}$ can arise from the temperature dependence of the *preexponential factor*. This point is detailed in ref. 39. Briefly, the (unimolecular) barrier-crossing frequency ν_n for the present systems appears to be determined at least partly by the dynamics of collective solvent polarization.[39,49,50] The rate of such "overdamped" solvent motion is expected to increase significantly with temperature, yielding an additional contribution to the rate-temperature dependence and thereby enhancing the Arrhenius activation energy. This component of $\Delta H_{ex}^{\ddagger}$ is labelled ΔH_{τ}^{*} in ref. 39. Dielectric continuum estimates of ΔH_{τ}^{*} in the present solvents are significant, ca 4.5 kJ mol^{-1}.[39] Consequently, the presence of this term can enlarge $\Delta H_{ex}^{\ddagger}$ so to offset the influence of noncontinuum effects.

Some comments along these lines can also usefully be made regarding the preexponential factors, A_{ex}, measured here (Tables IV, V). In the absence of the entropic and temperature-dependence dynamical factors noted above, we can express A_{ex} as[58]

$$A_{ex} = K_p \kappa_{el} \nu_n \qquad (6)$$

where K_p describes the statistical probability of forming the interfacial precursor state, and κ_{el} is the electronic transmission coefficient. In the absence of work terms ("double-layer effects"), we anticipate that $K_p \sim 0.1$ pm for electrochemical reactions.[58] The unimolecular frequency factors, $\kappa_{el}\nu_n$, extracted from the A_{ex} values by using Eq(6) in this fashion are also given in Table V. Listed alongside are inverse longitudinal relaxation times, τ_L^{-1}, for the three solvents; this quantity should roughly approximate $\kappa_{el}\nu_n$ in the continuum limit, and when the reaction is adiabatic (i.e., $\kappa_{el} \sim 1$).[49,50] Comparison between the $\kappa_{el}\nu_n$ and τ_L^{-1} values shows that the solvent-dependent

trends in the latter is roughly mimicked by the former quantity, although $\kappa_{el}\nu_n < \tau_L^{-1}$. The latter inequality has also been observed, to a greater extent, for metallocenium-metallocenium self-exchange reactions.[43] Most likely, it reflects a breakdown in one (or more) of the assumptions made above in applying Eq(6) to preexponential factors extracted from temperature-dependent kinetic data.

Finally, quite apart from the niceties of such kinetic data interpretations the present results (along with ref. 14) would appear to cast some doubt on the validity of the much larger k_s values, ca 200 cm s^{-1} reported for $Fc^{+/o}$ electrochemical exchange in acetonitrile.[15] It is possible that these measurements, although extremely elegant, suffered from difficulties associated with sealing the nanometer-sized microelectrodes.[14,60] The consequent deduction from these data of the presence of substantial reactant-electrode imaging effects[61] would also appear questionable at this point. In any event, the further pursuit of sub-ambient temperature conditions for evaluating rapid electrode kinetics using microelectrode voltammetric tactics would seem to be well worthwhile, especially for electrodes of varying dimensions.

ACKNOWLEDGMENT

We are grateful for the support of this work from the Office of Naval Research.

REFERENCES

1. R.M. Wightman, D.O. Wipf, in "Electroanalytical Chemistry – A Series of Advances", A.J. Bard, editor, Marcel Dekker, New York, Vol. 15, 1989, p.267
2. L.K. Safford, M.J. Weaver, J. Electroanal. Chem., 312 (1991), 69
3. R.P. Van Duyne, C.N. Reilley, Anal. Chem., 44 (1972), 142,153,158
4. A.M. Bond, R. Colton, Inorg. Chem., 15, (1976), 446
5. K.M. O'Connell, D.H. Evans, J. Am. Chem. Soc., 105 (1983), 1473
6. P. O'Brien, D.A. Sweigart, J. Chem. Soc. Chem. Comms., 86 (1986), 198
7. A.M. Bond, D.A. Sweigart, Inorg. Chim. Acta, 123 (1986), 167
8. W.J. Bowyer, D.H. Evans, J. Electroanal. Chem., 240 (1988), 227
9. W.J. Bowyer, D.H. Evans, J. Org. Chem., 53 (1988), 5234
10. B.E. Conway, M. Salomon, J. Chem. Phys., 41 (1964), 3169
11. B.E. Conway, D.J. Mackinnon, J. Electrochem. Soc., 116 (1969), 1655
12. U. Stimming, W. Schmickler, J. Electroanal. Chem., 150 (1983), 125
13. A. Matsunaga, K. Itoh, A. Fujeshima, K. Honda, J. Electroanal. Chem., 205 (1986), 343
14. A.S. Baranski, K. Winkler, W.R. Fawcett, J. Electroanal. Chem., 313 (1991), 367
15. R.M. Renner, M.J. Heben, T.L. Longin, N.S. Lewis, Science, 250 (1990), 1118
16. J.O. Howell, W.G. Kuhr, R.E. Ensman, R.M. Wightman, J. Electroanal. Chem., 209 (1986), 77
17. L.K. Safford, Ph.D. dissertation, Purdue University, 1991
18. M. Fleischmann, S. Pons, D.R. Rolison, P.P. Schmidt, "Ultramicroelectrodes", Datatech Systems, Inc., Morganton, NC, 1987
19. L.K. Safford, M.J. Weaver, J. Electroanal. Chem., 261 (1989), 241
20. A.R. Gowlay, S. McKee, J. Comp. Appl. Math, 3 (1977), 201
21. D. Shoup, A. Szabo, J. Electroanal. Chem., 160 (1984), 1

22. A.C. Michael, R.M. Wightman, C.A. Amatore, J. Electroanal. Chem., 267 (1989), 33

23. R.S. Nicholson, Anal. Chem., 37 (1965), 1351

24. A.J. Bard, L.R. Faulkner, "Electrochemical Methods", Wiley, New York, 1980, Chapter 6

25. M.E. Peover, J.S. Powell, J. Electroanal. Chem., 20 (1969), 427

26. W.R. Fawcett, A. Lasia, J. Phys. Chem., 82 (1978), 1114

27. J-M. Savéant, D. Tessier, Far. Disc. Chem. Soc., 74 (1982), 57

28. R.A. Peterson, D.H. Evans, J. Electroanal. Chem., 222 (1987), 129

29. W.J. Bowyer, E.E. Engelman, D.H. Evans, J. Electroanal. Chem., 262 (1989), 67

30. J. Newman, J. Electrochem. Soc., 113 (1966), 501

31. J.O. Howell, R.M. Wightman, Anal. Chem., 56 (1984), 524

32. C.P. Andrieux, D. Garreau, P. Hapiot, J. Pinson, J.M. Savéant, J. Electroanal. Chem., 243 (1988), 321

33. J.M. Savéant, D. Tessier, J. Phys. Chem., 81 (1977), 2192

34. D. Garreau, J.M. Savéant, D. Tessier, J. Phys. Chem., 83 (1979), 3003

35. R.A. Marcus, J. Chem. Phys., 43 (1965), 679

36. M.J. Weaver, F.C. Anson, J. Phys. Chem., 80 (1976), 1861

37. T. Gennett, M.J. Weaver, J. Electroanal. Chem., 186 (1985), 179

38. M.J. Weaver, T. Gennett, Chem. Phys. Lett., 113 (1985), 213

39. T. Gennett, D.F. Milner, M.J. Weaver, J. Phys. Chem., 89 (1985), 2787

40. G.E. McManis, M.N. Golovin, M.J. Weaver, J. Phys. Chem., 90 (1986), 6563

41. R.M. Nielson, M.J. Weaver, Organometallics, 8 (1989), 1636

42. R.M. Nielson, M.N. Golovin, G.E. McManis, M.J. Weaver, J. Am. Chem. Soc., 110 (1988), 1745

43. R.M. Nielson, G.E. McManis, M.N. Golovin, M.J. Weaver, J. Phys. Chem., 92 (1988), 3441

44. R.M. Nielson, G.E. McManis, L.K. Safford, M.J. Weaver, J. Phys. Chem., 93 (1989), 2152

45. R.M. Nielson, G.E. McManis, M.J. Weaver, J. Phys. Chem., 93 (1989), 4703

46. G.E. McManis, R.M. Nielson, A. Gochev, M.J. Weaver, J. Am. Chem. Soc., 111 (1989), 5533

47. M.J. Weaver, G.E. McManis, W. Jarzeba, P.F. Barbara, J. Phys. Chem., 94 (1990), 1715

48. A.M. Kuznetsov, D.K. Phelps, M.J. Weaver, Int. J. Chem. Kinetics, 22 (1990), 815

49. M.J. Weaver, G.E. McManis, Acc. Chem. Res., 23 (1990), 294

50. M.J. Weaver, Chem. Rev., in press

51. D.K. Phelps, A.A. Kornyshev, M.J. Weaver, J. Phys. Chem., 94 (1990), 1454

52. P.G. Dzhavakhidze, A.A. Kornyshev, L.I. Krishtalik, J. Electroanal. Chem., 228 (1987), 329

53. C. Creutz, Prog. Inorg. Chem., 30 (1983), 1

54. M.J. Powers, T.J. Meyer, J. Am. Chem Soc., 100 (1978), 4393

55. R.L. Blackbourn, J.T. Hupp, J. Phys. Chem., 94 (1990), 1788

56. G.E. McManis, A. Gochev, R.M. Nielson, M.J. Weaver, J. Phys. Chem., 93 (1989), 7733

57. J.T. Hupp, M.J. Weaver, J. Phys. Chem., 88 (1984), 1860

58. J.T. Hupp, M.J. Weaver, J. Electroanal. Chem., 152 (1983), 1

59. Krishnaji, A. Mansingh, J. Chem. Phys., 41 (1964), 827

60. A.S. Baranski, J. Electroanal. Chem., 307 (1991), 287

61. R.A. Marcus, J. Phys. Chem., 95 (1991), 2010

TABLE I Temperature-dependent resistivities, ρ, for electrolyte solutions[a]

T/K	Acetone[b]	Propionitrile[c]	Butyronitrile[c,d]	Acetonitrile[c,d]
338		62.9		
318		80.9		39.4
298	75.2	104	127 (123)	52.1 (49.7)
278	101	147	159 (153)	64.9 (62.7)
258	136	207	231 (224)	94.2 (85.2)
238	212	303	357 (349)	
218	332	509	602 (591)	
198	584	915	1124 (1112)	
$\Delta H_\rho^\ddagger$ kJ mol^{-1}	10.0[e]	10.6[e]	10.8 (11.3)[e]	9.7 (9.3)[e]

[a] Obtained by ac impedance (50-500 Hz) at 1 cm diameter Au disk electrode. Values generally reproducible to ±1-2%

[b] Contained 0.3 M tetraethylammonium hexafluorophosphate (TEAH)

[c] Contained 0.3 M tetrabutylammonium hexafluorophosphate (TBAH)

[d] Values in parentheses obtained by temperature interpolation from data given in ref. 29

[e] Obtained from (Arrhenius) slope of plot of $R \ln \rho$ vs. (1/T)

TABLE II Temperature-dependent diffusion coefficients[a], D x 10^5 cm^2 s^{-1}, for reactants in media employed here.

T/K	Acetone[b]	Propionitrile[c]			Butyronitrile[c]		
	$Fc^{+/o}$	$Fc^{+/o}$	o-$Nt^{o/-}$	$Nm^{o/-}$	$Fc^{+/o}$	o-$Nt^{o/-}$	$Nm^{o/-}$
298	2.0	1.8	2.3	2.5	0.87	1.9	1.7
278	1.3	1.2	1.5	1.6	0.68	1.2	1.1
258	1.0	0.97	1.2	1.1	0.52	0.81	0.69
238	0.71	0.68	0.61	0.77	0.37	0.51	0.45
218	0.45	0.40	0.32	0.35	0.18	0.24	0.24
198	0.28	0.21			0.09		
$\Delta H_D^{\ddagger}$	9.4[d]	10.6[d]	13.2[d]	13.0[d]	10.7[d]	13.7[d]	12.5[d]

[a] Obtained from diffusion-limited current of steady-state voltammogram for oxidation of ferrocene, and reduction of o-nitrotoluene and nitromesitylene at a 5 μm radius Au microdisk, by means of Eq(2)

[b] Supporting electrolyte was 0.3 M TEAH

[c] Supporting electrolyte was 0.3 M TEAH

[d] Arrhenius activation enthalpy for diffusion, obtained from slope of plot of RlnD vs. (1/T)

TABLE III Additional voltammetric peak separation due to finite electrode kinetics, $\Delta(\Delta E_p)_k$ (mV), for ferrocenium–ferrocene and o-nitrotoluene$^{o/-}$ couples at 298K and 198K.

	Ferrocenium–Ferrocene[d]						o-Nitrotoluene$^{o/-}$[e]			
ν/Vs^{-1}[a]	Acetone[b]		Propionitrile[c]		Butyronitrile[c]		Propionitrile[c]		Butyronitrile[c]	
	298K	198K	298K	198K	298K	198K	298K	198K	298K	198K
1×10^4	19		29		66		121		127	
5×10^3	12		23		53		85		104	
2×10^3	6	111	17	100	31	170	67		74	
1×10^3	5	89	14	87	21	145	41	220	51	204
500	4	72	9	71	18	111	36	196	43	187
200		49				94		163		158
100		36				73		144		132

[a] Voltammetric sweep rate

[b] Contained 0.3 M TEAH supporting electrolyte

[c] Contained 0.3 M TBAH supporting electrolyte

[d] Reactant (ferrocene) concentration was 3 mM

[e] Reactant (o-nitrotoluene) concentration was 3.5 mM

TABLE IV Temperature-dependent standard electrochemical rate constants, k_s (cm s^{-1}), for ferrocenium–ferrocene ($Fc^{+/o}$), o-nitrotoluene$^{o/-}$ (o-$Nt^{o/-}$), and nitromesitylene$^{o/-}$ ($Nm^{o/-}$) redox couples at Au–nonaqueous interfaces.

T/K	Acetone[a]	Propionitrile			Butyronitrile		
	$Fc^{+/o}$	$Fc^{+/o}$	o-$Nt^{o/-}$	$Nm^{o/-}$	$Fc^{+/o}$	o-$Nt^{o/-}$	$Nm^{o/-}$
298	≈ 5.5	3.0	0.75	0.36	0.95	0.58	0.31
278	2.5	2.1	0.36	0.19	0.48	0.28	0.16
258	1.4	0.68	0.16	0.075	0.36	0.12	0.082
238	0.92	0.43	0.071	0.029	0.17	0.042	0.025
218	0.38	0.15	0.014		0.04	0.014	
198	0.083	0.07			0.02		
$\Delta H^{\ddagger}_{ex}$, kJ mol^{-1}[c]	19.5	19	26	25.5	19.5	25	25.5
A_{ex}, cm s^{-1}	1.5×10^4	6×10^3	3×10^4	1.0×10^4	2.5×10^3	1.5×10^4	9×10^3

[a] Contained 0.3 M TEAH supporting electrolyte

[b] Contained 0.3 M TBAH supporting electrolyte

[c] Arrhenius activation enthalpy for electrochemical exchange, obtained from slope of plot of R ln k_s vs 1/T

[d] Arrhenius preexponential factor, obtained from $\Delta H^{\ddagger}_{ex}$ and k_s by using Eq(4)

TABLE V Comparison of Rate Parameters for Ferrocenium–Ferrocene Electrochemical Exchange with Simple Theoretical Predictions

Solvent	k_s[a] cm s^{-1}	$\Delta H_p^{\ddagger}$[a] kJ mol^{-1}	ΔG^{*}_{cont}[b] kJ mol^{-1}	A_{ex}[a] cm s^{-1}	$\kappa_{el}\nu_n$[c] s^{-1}	τ_L^{-1}[d] s^{-1}
Acetone	~5.5	19.5	24	1.5×10^4	1.5×10^{12}	4×10^{12}
Propionitrile	3.0	19	24.5	6×10^3	6×10^{11}	$\sim 4 \times 10^{12}$
Butyronitrile	0.95	19.5	23.5	2.5×10^3	2.5×10^{11}	$\sim 1.5 \times 10^{12}$

[a] Experimental values taken from Table IV

[b] Activation free energy for electrochemical exchange, extracted from dielectric continuum model [Eq(5)] together with inner-shell component as outlined in the text

[c] Effective unimolecular frequency factor, extracted from A_{ex} values by using Eq(6) with $K_p = 0.1$ pm (see text)

[d] Inverse solvent longitudinal relaxation times at ca 25°C, extracted from sources quoted in ref. 46 (for acetone, propionitrile) and from ref. 59 (for butyronitrile)

FIGURE CAPTIONS

Fig. 1

Cathodic-anodic peak potential separations, ΔE_p (V), for simulated one-electron cyclic voltammograms at a 5 μm radius microelectrode as a function of temperature, T(K), showing typical effects of solution resistance and finite electrode kinetics. Common parameters (see text); $\nu = 10^3$ V s^{-1}, $C_{dl} = 16$ μF cm^{-2}, $C^\circ = 1$ m$\underline{M}$. Dotted curve is ΔE_p in the complete absence of resistance and finite kinetic effects. Dashed curve refers to $\rho = 140$ ohm cm at 298K, and effective temperature dependence, $\Delta H_\rho^\ddagger = 15$ kJ mol^{-1}; diffusion coefficient $D = 1 \times 10^{-5}$ cm^2 s^{-1} at 298K, $\Delta H_D^\ddagger = 15$ kJ mol^{-1}. Solid traces refer to the additional presence of finite electrode kinetics, with $k_s = 5$ cm s^{-1} at 298K, and $\Delta H_{ex}^\ddagger = 40, 25$, and 10 kJ mol^{-1} in a-c, respectively.

Fig. 2

Simulated voltammetric peak separations, ΔE_p (V), versus $\log(\nu^{-\frac{1}{2}})$ where ν is the scan rate (V s^{-1}), obtained at 298K (curves a,b) and 198K (curves c-f) in the presence of solution resistance and finite electrode kinetics, with parameters as in Fig. 1. Curves a,c: for $k_s \rightarrow \infty$. Curve b, $k_s = 5$ cm s^{-1}. Curves d-f, $k_s = 0.65$, 0.02, and 7×10^{-4} cm s^{-1}, respectively (i.e., corresponding to $\Delta H_{ex}^\ddagger = 10$, 25, and 40 kJ mol^{-1}, respectively).

Fig. 3

Simulated voltammograms at 5 μm radius electrode over range of temperatures from 298K (outermost trace) to 198K. Parameters: $\nu = 10^3$ V s^{-1}, $C_{dl} = 15$ μF cm^{-2}, $C^\circ = 1$ m$\underline{M}$, $D = 10^{-5}$ cm^2 s^{-1} (298K), $\Delta H_D^\ddagger = 15$ kJ mol^{-1}, $\rho = 140$ ohm cm (298K), $\Delta H_\rho^\ddagger = 15$ kJ mol^{-1}, $k_s = 5$ cm s^{-1} (298K), $\Delta H_{ex}^\ddagger = 20$ kJ mol^{-1}.

Fig. 4

Experimental voltammetric peak separations, ΔE_p (V), at 5 μm radius gold electrode versus temperature, T(K), at 10^3 V s^{-1} for 3 m$\underline{M}$ ferrocene (circles), 3.5 m$\underline{M}$ o-nitrotoluene (squares), and 3.5 m$\underline{M}$ nitromesitylene (triangles) in butyronitrile with 0.3 $\underline{M}$ TBAH. Dashed curve is approximate response simulated in the absence of finite electrode kinetics (i.e., for $k_s \rightarrow \infty$).

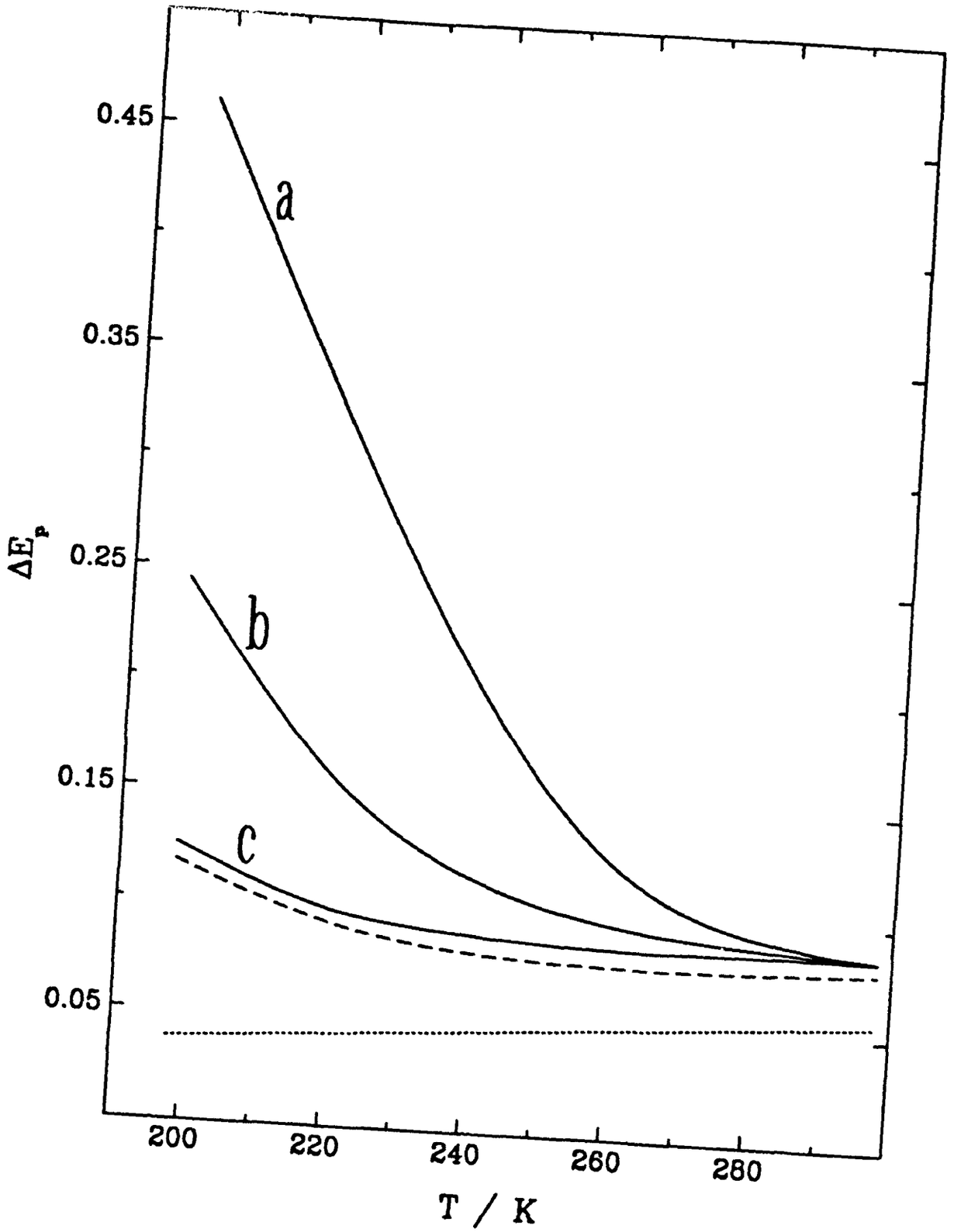

FIG 1

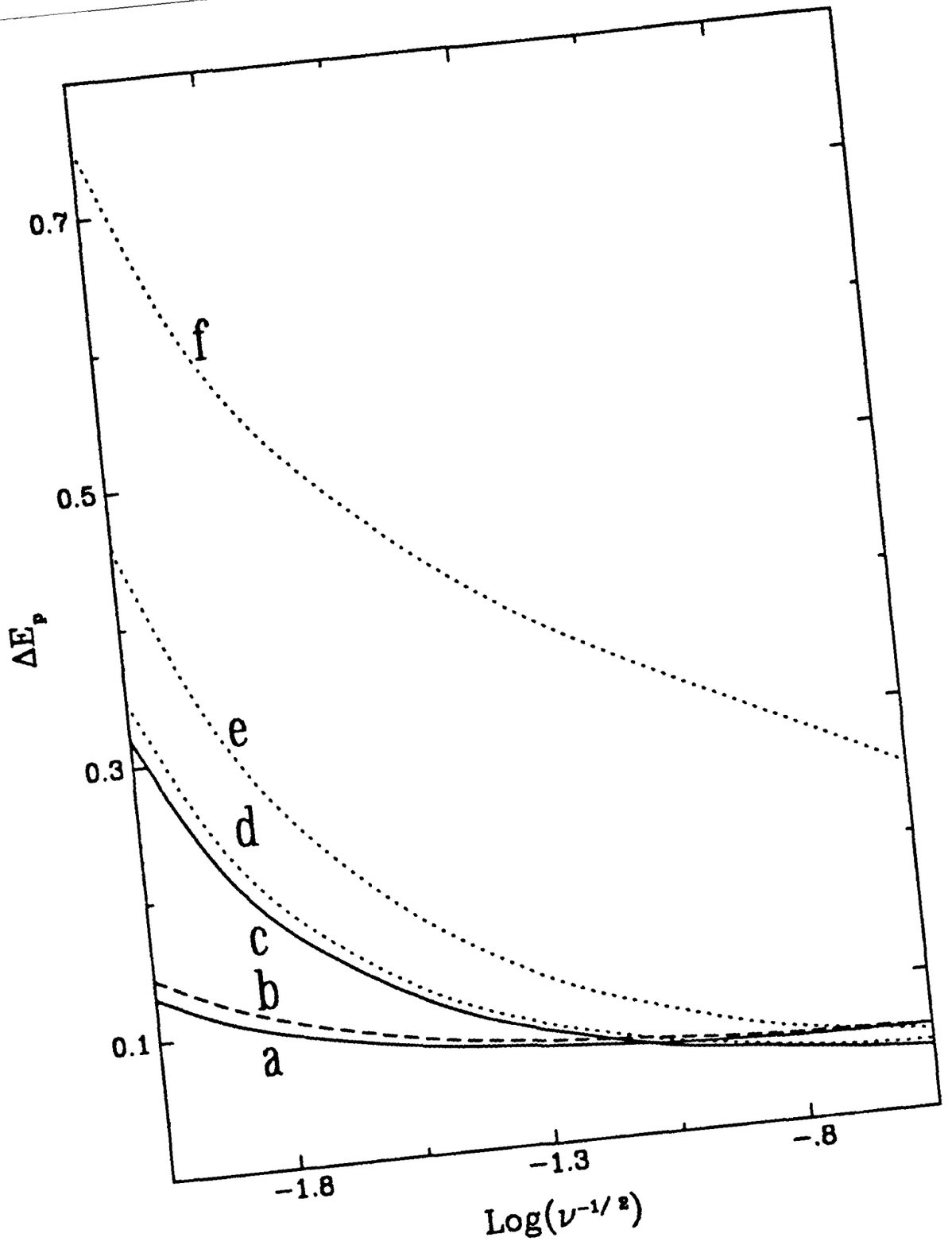

FIG 2

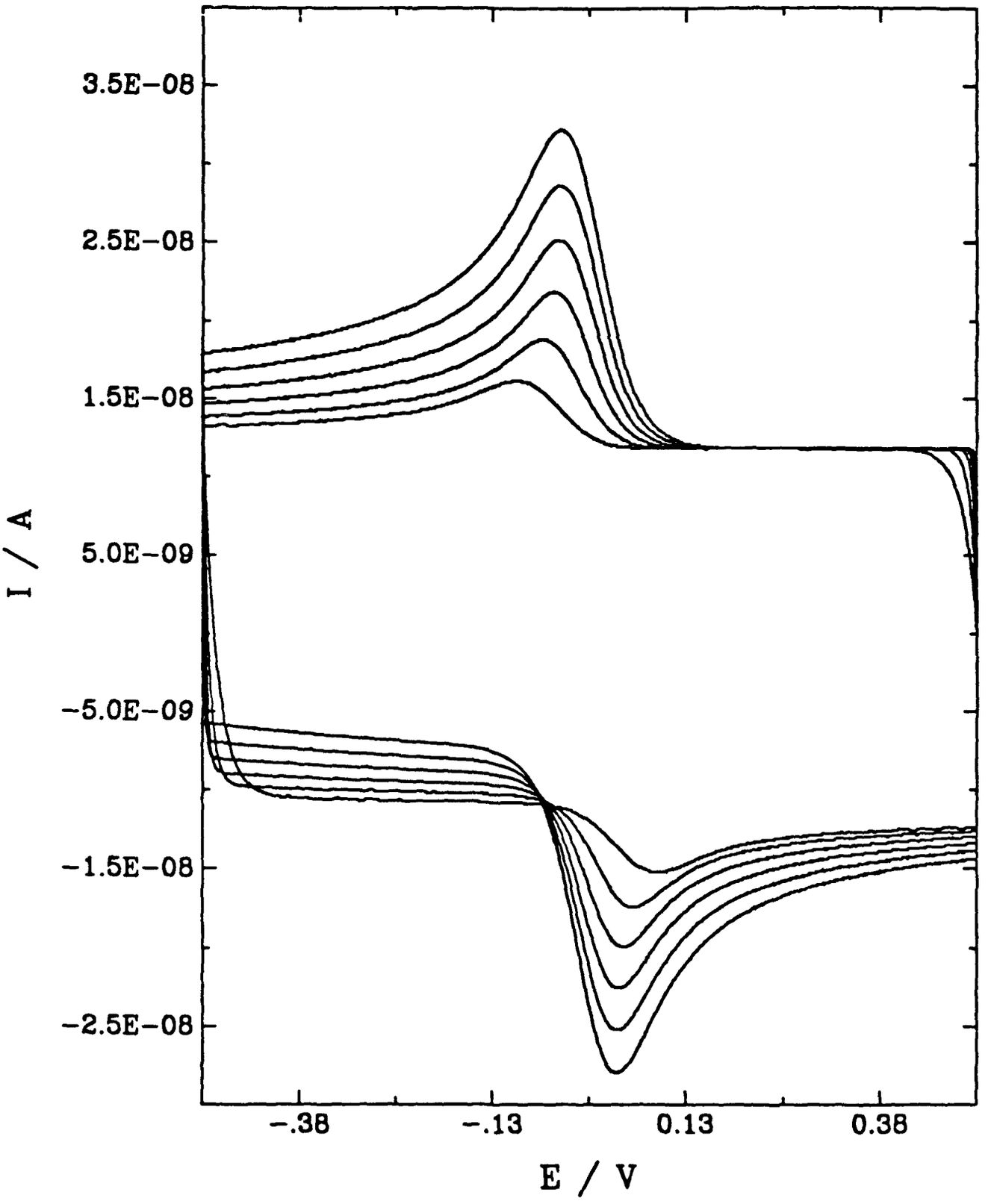

FIG 3

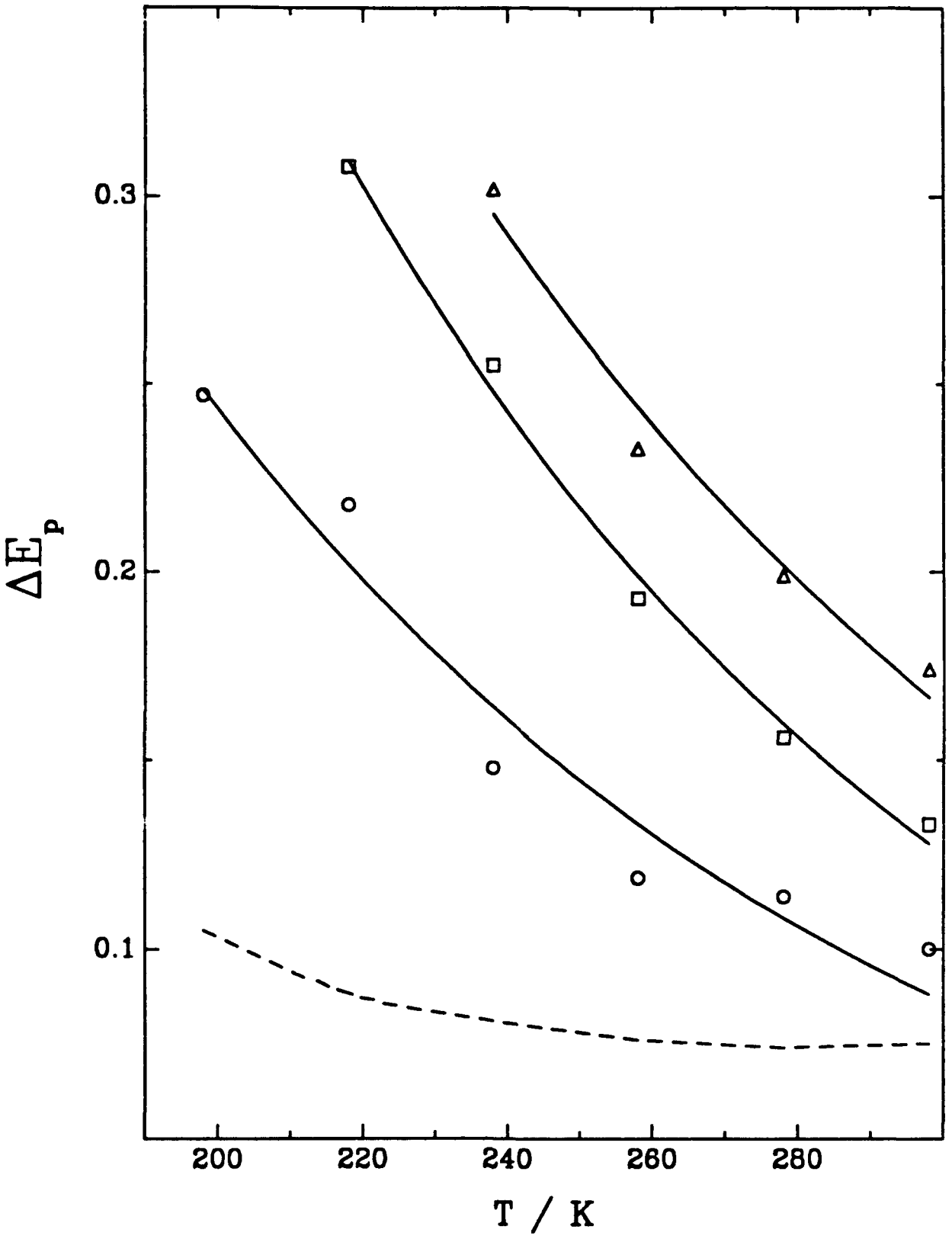

FIG 4